Received: 11 June 2019 | Revised: 16 October 2019 | Accepted: 2 November 2019

DOI: 10.1002/mgg3.1082

Molecular Genetics & Genomic Medicine Open Access WILEY

ORIGINAL ARTICLE

Novel *FSHR* variants causing female resistant ovary syndrome

Shuzin Khor | **Qifeng Lyu** | **Yanping Kuang** | **Xuefeng Lu**

Department of Assisted Reproduction, Shanghai Ninth People's Hospital, Shanghai Jiaotong University School of Medicine, Shanghai, China

Correspondence
Xuefeng Lu and Yanping Kuang, Department of Assisted Reproduction, Shanghai Ninth People's Hospital, Shanghai Jiaotong University School of Medicine, 639 Zhizaoju Rd, Shanghai 200001, China
Email: xuefenglu126@126.com (X. L.) and kuangyanp@126.com (Y. K.)

Funding information
National Natural Science Foundation of China, Grant/Award Number: 81873856 and 81771533; Clinical Research Program of the 9th People's Hospital, Shanghai Jiao Tong University School of Medicine, Grant/Award Number: JYLJ035

Abstract

Background: Pathogenic variants of follicle-stimulating hormone receptor (FSHR) are known to cause amenorrhea and infertility in women. However, only a limited number of pathogenic *FSHR* variants have been reported, and few reports described detailed characteristics of patients with pathogenic *FSHR* variants.

Methods: The affected siblings and both parents were subjected to whole-genome exon sequencing. Transient transfection of HEK 293T cells was performed with constructed vectors. The cellular localization of the FSHR protein was evaluated using confocal microscopy, and cyclic adenosine monophosphate (cAMP) production was detected with a cAMP ELISA kit.

Results: A Chinese family with two siblings carrying compound heterozygous pathogenic variants of *FSHR*: c.182T>A (p.Ile61Asn) and c.2062C>A (p.Pro688Thr). Both siblings had amenorrhea, infertility, and resistance to gonadotropin (Gn) stimulation but showed high anti-Müllerian hormone levels and early antral follicles. Molecular dynamics simulations of the FSHR variants revealed significant changes in structural characteristics and electrostatic potential. In vitro analysis indicated that the p.Ile61Asn variant lacked cell surface localization and completely abolished the cAMP second messenger response. The p.Pro688Thr variant retained cell surface localization but caused decreased FSH-induced cAMP production.

Conclusion: We found two novel pathogenic *FSHR* variants causing resistant ovarian syndrome. This study expands the genotypic spectrum of pathogenic *FSHR* variants and our knowledge of phenotype–genotype correlations.

KEYWORDS
female infertility, FSHR, pathogenic variants, resistant ovary syndrome

1 | INTRODUCTION

Primary ovarian insufficiency (POI) is defined as primary or secondary amenorrhea before the age of 40 with hypoestrogenism and serum follicle-stimulating hormone (FSH) levels > 40 mIU/ml. Resistant ovary syndrome (ROS) is proposed as a special form of POI characterized by the hypersecretion of gonadotropins (Gns), the presence of normal primordial follicles in ovarian biopsies, a normal antral follicle count (AFC) by ultrasound scan, normal anti-Müllerian hormone (AMH) levels, and resistance to Gn stimulation. ROS, also known as Savage syndrome, was first reported by Jones GS et al. in 1969 (Jones & De Moraes-Ruehsen, 1969), but the mechanism of ROS is still unclear. The FSH receptor (FSHR) (MIM:136,435; GenBank: NM_000145.4) is expressed in granulosa cells and is thought to tightly regulate

the various phases of follicle maturation in response to periodic pituitary FSH release. FSHR belongs to a structurally unique glycoprotein hormone receptor subfamily of G protein-coupled receptors (GPCRs) with an exceptionally long extracellular domain (ECD), seven transmembrane domains, three short intracellular loops, three extracellular loops, and an intracellular tail (Jiang et al., 2012). Dimeric FSH binds to the ectodomain of FSHR according to a hand-clasp model, which triggers a conformational change in FSHR and subsequently activates G protein and adenylyl cyclase, resulting in increased cyclic adenosine monophosphate (cAMP) production.

In 1995, Aittomäki K et al reported the first pathogenic *FSHR* variant, p.Ala189Val, in the Finnish population (Aittomaki et al., 1995). The p.Ala189Val variant, located in the ECD of FSHR, disrupts membrane targeting and markedly impairs FSHR function in vitro. Women with the p.Ala189Val variant show primary/secondary amenorrhea, normal-sized ovaries, and high serum FSH levels. Histological examination of the ovaries of affected women revealed normal follicular development up to the small antral stage and disruption at later stages, indicating a distinct form of ovarian insufficiency resulting from FSH resistance rather than follicular depletion (Aittomaki et al., 1996). AMH is secreted by ovarian granulosa cells of growing ovarian follicles from the primary to the small antral stage, and its serum levels reflect ovarian follicle reserves. Accordingly, patients with the p.Ala189Val variant exhibit low to normal AMH levels that are higher than those in women with ovarian insufficiency (Kallio et al., 2012). P.Ala189Val variant is particularly prevalent in the Finnish population; it has not been detected in women with a similar phenotype in various other countries.

Following the report of the p.Ala189Val variant, a few other pathogenic FSHR variants were reported, including p.Arg59*, p.Ile160Thr, p.Asp191Ile, p.Val221Gly, p.Asp224Val, and p.Pro348Arg in the ECD (Allen et al., 2003; Beau et al., 1998; Liu et al., 2017; Nakamura, Maekawa, Yamagata, Tamura, & Sugino, 2008; Touraine et al., 1999); p.Asp408Tyr, p.Ile418Ser, p.Pro587His, and p.Ala419Thr in the transmembrane domain (Bramble et al., 2016; Doherty et al., 2002; Katari et al., 2015; Kuechler et al., 2010); p.Pro519Thr and p.Leu601Val in the extracellular loop (Allen et al., 2003; Touraine et al., 1999); and p.Arg573Cys in the intracellular loop (Beau et al., 1998). However, no pathogenic variant in the intracellular tail of FSHR have been reported in POI/ROS patients. Moreover, only a proportional phenotypic description of the patients with identified pathogenic *FSHR* variants has been provided, without AMH detection or histological biopsy analysis. However, histological biopsy analysis was performed in patients carrying the homozygous pathogenic *FSHR* variants p.Arg59*, p.Ala189Val, and p.Pro519Thr and compound heterozygous pathogenic *FSHR* variants, including p.Ile160Thr and p.Arg573Cys or p.Asp224Val and p.Leu601Val; the results revealed the presence of normal follicular development up to the small antral stage and disruption at later stages. AMH levels vary from 0.13 to 7.82 ng/ml in patients with the p.Ala189Val and p.Asp408Tyr variants. AMH levels have not been reported in other patients with pathogenic *FSHR* variants. Consistent with the characteristics of patients with pathogenic *FSHR* variants, Fshr-/- KO female mice show sterility, elevated serum Gn levels and low oestradiol (E2) levels. Histological examination revealed primordial, primary, and secondary follicles but no antral follicles (Dierich et al., 1998).

Genetic analysis of the families of ROS patients will help elucidate the mechanism of ROS and the function of FSHR. In this study, we evaluated a family in which the proband and her elder sister are affected by ROS caused by inactivating compound heterozygous pathogenic *FSHR* variants, c.182T>A (p.Ile61Asn) and c.2062C>A (p.Pro688Thr), that have not been previously reported in ROS patients. Detailed characteristics of these patients are described herein. These findings add to the molecular diagnostic tools for ROS, extend our understanding of extracellular and intracellular events as well as signal transduction in response to FSH, and are helpful for establishing a correlation between genotype and clinical phenotype.

2 | MATERIALS AND METHODS

2.1 | Ethical compliance

This study was approved by the Ethics Committee (Institutional Review Board) of the Ninth People's Hospital of Shanghai. All patients received a briefing about the study and provided informed consent.

2.2 | Subjects

The proband (II-3) is a 27-year-old female who was referred to the assisted reproductive technology (ART) center of this hospital due to primary infertility (Figure 1). She exhibited secondary amenorrhea after one menstrual cycle (Table 1). Until she began hormone replacement therapy (HRT) at 21 years of age, her menstrual cycle was regular, and her breasts developed from Tanner stage I to Tanner stage II. Laboratory evaluation revealed the following hormone levels: FSH 84.95 mIU/ml, luteinizing hormone (LH) 65.24 mIU/ml, E2 17.0 pg/ml, and AMH 7.07 ng/ml (Table 1). The proband has two sisters. Her eldest sister is healthy and had given birth to one daughter and one son. Her elder sister is 30 years old and has primary amenorrhea and infertility; her menstrual cycle was induced by HRT at

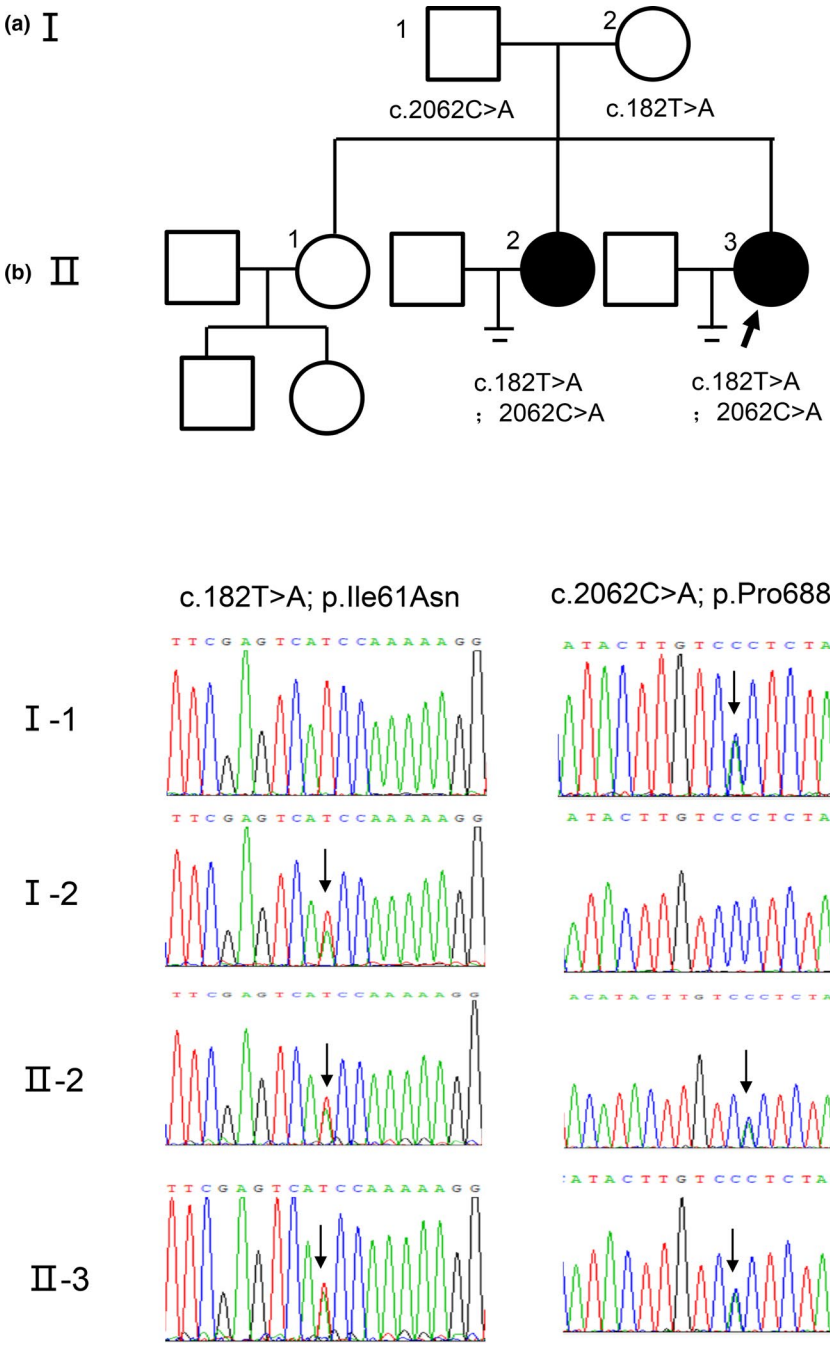

FIGURE 1 Identification of novel variants, c.182T>A (p.Ile61Asn) and c.2062C>A (p.Pro688Thr), in the *FSHR*. (a) Pedigree of the resistant ovary syndrome (ROS) patient. The proband is indicated by an arrow. (b) Sanger sequencing confirmed the compound heterozygous variants in the subjects and the homozygous status of their parents

20 years of age, and laboratory evaluation revealed the following hormone levels: FSH 94.58 mIU/ml, LH 67.1 mIU/ml, E2 22 pg/ml, and AMH 13.84 ng/ml (Table 1). A physical examination revealed normal external female genitalia, pubic hair, and female breast development in the patient. Both the proband and her elder sister presented small ovaries, with 5–6 follicles at the early antral stage (2–3 mm at ultrasonography). Exogenously administered human Gns failed to induce follicle development and ovulation in the proband and her elder sister. Both women displayed a 46, XX karyotype. Their mother had regular menses and underwent menopause at the age of 46. Both of their parents were healthy and had no history of difficulty conceiving.

2.3 | DNA sequencing

All genomic DNA samples from the patients, family members, and controls were extracted from peripheral blood using standard methods. We sequenced the exomes of all family members using Agilent SureSelect Whole-exome capture and Illumina sequencing technology (Feng et al., 2016).

Only variants with minor allele frequency of less than 1% were considered to be pathogenic. Variants cosegregated with the disease phenotype in this family were then filtered and considered as disease causing pathogenic variants, according to the NHLBI (National Heart, Lung, and Blood Institute)

TABLE 1 Clinical characteristics of affected individuals

Patients	Age (years)	External genitalia	Pubic hair and breast development	Menstrual cycles	Fertility	Basal FSH (mIU/ml; normal range: 3.03–8.08 mIU/ml)	Basal LH (mIU/ml; normal range: 1.80–11.78 mIU/ml)	Basal E2 (pg/ml; normal range:>21 pg/ml)	AMH (ng/ml; normal range: 1.75–4.46 ng/ml)	Pelvic ultrasound
Elder sister (II–2)	30	Normal	Normal	Primary Amenorrhea	Absence of ovulation	94.58	67.1	22	13.84	Small sized ovaries with 5–6 follicles at the early antral stage
The proband(II–3)	27	Normal	Normal	Secondary Amenorrhea	Absence of ovulation	84.95	65.24	17	7.07	Small sized ovaries with 5–6 follicles at the early antral stage

Exome Sequencing Project database (http://evs.gs.washington.edu/EVS/) and the Exome Aggregation Consortium. Mutations in FSHR were validated by Sanger sequencing with a 3730XL sequencer (Applied Biosystems) according to the manufacturer's instructions.

2.4 | Endocrine assays

Serum FSH, LH, E2, and progesterone (P) levels were measured by chemiluminescence (Abbott Biologicals B.V., Weesp, Netherlands). The lower limits of sensitivity were as follows: FSH, 0.06 mIU/ml; LH, 0.09 mIU/ml; E2, 10.0 pg/ml; and P, 0.1 ng/ml. The AMH level was measured by an automated Access AMH assay (Beckman Coulter, Inc.) (normal range: 1.75–4.46 ng/ml).

2.5 | Cell culture

Human embryonic kidney cells (HEK-293T) were cultured in complete Dulbecco's modified Eagle's medium (DMEM; Gibco) with 10% fetal bovine serum (HyClone) at 37°C in a humidified incubator in an atmosphere containing 5% CO_2.

2.6 | Molecular cloning and expression of wild-type FSHR and FSHR variants

Wild-type human *FSHR* cDNA (NM_000145) was synthesized (General Biotech) and cloned into the GV141 vector (Genechem) to create the fusion protein expression vector pFSHR-3Flag. The sequences encoding p.Ile61Asn and p.Pro688Thr were amplified from the pFSHR-3Flag vector using a high-fidelity DNA polymerase (New England Biolabs). The following oligonucleotides were employed for mutagenesis: FSHR/ p.Ile61Asn P1, 5′-TGTCCTCACCAAGCTTCGAGTCAACCAAAAAGGTGCATTTTCAGGATTTGGG-3′; FSHR/ p.Ile61Asn P2, 5′-CCCAAATCCTGAAAATGCACCTTTTTGGTTGACTCGAAGCTTGGTGAGGACA-3′; FSHR/ p.Pro688Thr P1: 5′-CAGCTCCCAGAGTCACCAATGGTTCCACTTACATAC-3′; and FSHR/ p.Pro688Thr P2: 5′-GTATGTAAGTGGAACCATTGGTGACTCTGGGAGCTG-3′. These constructs were transiently transfected into HEK-293T cells using Lipofectamine® 2000 (Invitrogen). Expression was verified by Western blotting.

2.7 | Ovarian biopsy and histological analysis

Biopsies from both ovaries of the proband were taken by laparoscopy. Visual examination revealed a small uterus and two small, gray ovaries without any growing follicles or a corpus luteum,

which was consistent with the ultrasound imaging results. A small (8 mm^3) piece of tissue was extracted from each ovary.

Histological sections were prepared from tissue fixed in formalin and embedded in paraffin wax. Hematoxylin and eosin were used as general stains following standard procedures. Morphology was observed under a microscope (Olympus).

2.8 | Simulation system setup

Based on the known sequence of wild-type FSHR (FSHR/WT), a corresponding structural model was built using I-Tasser (Yang et al., 2015) referring to the ectodomain crystal structure (PDB ID: 4AY9)(Jiang et al., 2012). Protein coordinates were preoriented to the membrane-binding situation with the orientations of proteins in membranes database (Lomize, Pogozheva, Joo, Mosberg, & Lomize, 2012). Then, CHARMM-GUI Membrane Builder was employed to construct a simulation model in which FSHR was located on 1,2-dioleoyl-sn-glycero-phosphocholine (DOPC) (Jo, Kim, Iyer, & Im, 2008; Lee et al., 2016; Wu et al., 2014). With the help of Discovery Studio 2017 R27, the isoleucine at position 61 was mutated to asparagine (c.182T>A [p.Ile61Asn]), and the proline at position 688 was mutated to threonine (c.2062C>A[p.Pro688Thr]). Finally, the structures of FSHR/WT, p.Ile61Asn, and p.Pro688Thr were taken as the starting structures for molecular dynamics (MD) simulations.

2.9 | MD simulations

The force field parameters of the systems were calculated based on the Amber ff14SB force field (for proteins) (Maier et al., 2015), Amber Lipid14 force field (for lipids) (Dickson et al., 2014), and the general amber force field (GAFF) (Wang, Wolf, Caldwell, Kollman, & Case, 2004). Thereafter, the complexes were solvated in a TIP3PBOX water model with Na^+ and Cl^- at 0.15 mol/L.

Energy minimization was performed first in the MD simulations. Initially, the positions of FSHR were restrained, and the energy of lipids, water, and counterions was minimized for 10 ps. Next, the position of each atom in the system was relaxed for 20 ps. Then, the systems were subjected to heating from 0 to 300 K over 300 ps in a canonical ensemble (NVT). Next, 700-ps equilibration runs for the systems were performed in NVT. Finally, 2-ns MD simulations were carried out for the complexes and structures.

Periodic boundary and NPT conditions were used in the simulations. Long-range electrostatic forces were analyzed by the particle-mesh Ewald (PME) method, and a cutoff of 10 Å was employed to simplify both the short-range electrostatic force and the van der Waals force. Covalent bonds involving hydrogen were restricted via the SHAKE method.

2.10 | Western blotting

Transfected HEK-293T cells were lysed in radioimmunoprecipitation assay buffer (50 mmol/L Tris-HCl, 150 mmol/L NaCl, 1% Triton X-100, 0.1% SDS, and 1% deoxycholic acid sodium) and sonicated. The supernatant from the clarified lysate was immediately snap-frozen and stored at −80°C. The protein samples from transfected HEK-293T cells were separated by SDS-PAGE and subjected to Western blotting analysis with a monoclonal anti-Flag antibody (1:3,000, Sigma), an anti-GAPDH antibody (1:2000, Santa Cruz Biotechnology), and horseradish peroxidase-conjugated goat anti-mouse IgG (1:2000, Santa Cruz Biotechnology).

2.11 | Immunofluorescence assay

HEK-293T cells were transiently transfected with the FSHR-3Flag, p.Ile61Asn-3Flag and p.Pro688Thr-3Flag vectors using Lipofectamine® 2000 (Invitrogen). The transfected cells were cultured for 48 hr and then fixed with 4% paraformaldehyde for 20 min. The fixed cells were stained with a monoclonal anti-Flag antibody (1:200, Sigma), Alexa Fluor 488-labeled donkey anti-mouse IgG H&L (1:1,000, Abcam), and the nuclear marker 4′,6-diamidino-2-phenylindole (DAPI; Sigma). Images were acquired using a confocal microscope (Zeiss LSM 710, Oberkochen).

2.12 | Functional analysis of the FSHR variants

HEK293T cells were transiently transfected with the FSHR-3Flag, p.Ile61Asn-3Flag and p.Pro688Thr-3Flag vectors using Lipofectamine® 2000 (Invitrogen). Forty-eight hours later, the cells were washed twice with serum-free DMEM (Gibco) and then incubated with increasing concentrations of FSH (0–500 ng/ml, Sigma). The total cAMP concentration in each well was measured with a specific ELISA kit (R&D Systems). The experiments were repeated three times, and the results are presented as the mean ± *SEM*.

3 | RESULTS

3.1 | Pathogenic *FSHR* variants

After whole-exome sequencing, bioinformatics filtering analysis, and homozygosity mapping, *FSHR* was the only gene that segregated with the phenotype of the proband and her elder sister. Sanger sequencing of the parents and two affected daughters confirmed two variants in *FSHR* (c.182T>A[p.Ile61Asn] and c.2062C>A[p.Pro688Thr]),

which indicated an autosomal recessive model of inheritance. The c.2062C>A (p.Pro688Thr) variant has not been previously reported, and the c.182T>A (p. Ile61Asn) has an allele frequency of ~0.001651% according the Exome Aggregation Consortium (exac.-broadinstitute.org). Parent I-1 is a heterozygous (wild-type/c.2062C>A [p.Pro688Thr]) carrier as shown by overlapping C and A peaks at site 2062 of the *FSHR* . Parent I-2 is a heterozygous (wild-type/c.182T>A [p. Ile61Asn]) carrier as shown by overlapping T and A peaks at site 182 of the *FSHR*. Both affected daughters, II-2 and II-3, harbor compound heterozygous *FSHR* variants, c.182T>A[p.Ile61Asn] and c.2062C>A[p.Pro688Thr], in exons 2 and 10 of the *FSHR*, respectively (Figure 1b). Their unaffected older sister (II-1) did not carry any variants of *FSHR*. Based on the ROS phenotype of both affected siblings, we considered the compound heterozygous pathogenic *FSHR* variants (c.182T>A[p.Ile61Asn] and c.2062C>A[p.Pro688Thr]) to be the cause of ROS.

3.2 | Ovary structure

Through ultrasound, we found that the proband and her elder sister had small bilateral ovaries, with 5–6 small antral follicles (diameter: 2–3 mm) each, even after exogenous Gn stimulation (Figure 2a). Representative biopsies were taken from both ovaries of the proband (II-3); microscopy revealed a compact stroma containing numerous primordial follicles and a few primary follicles with granulosa cells. However, secondary follicles, corpora lutea, and mature Graafian follicles were absent (Figure 2b). These ovarian characteristics are markedly different from those of patients with ovarian insufficiency. These results indicated that follicle development and maturation were arrested in these patients, which caused amenorrhea and infertility.

3.3 | Molecular modeling of FSHR variants

To further investigate how the c.182T>A (p.Ile61Asn) and c.2062C>A (p.Pro688Thr) variants disrupt FSHR function, we constructed a three-dimensional model using the homology modeling method. N61, which possesses strong polarity, widens the distance between extracellular loops. Thus, in the presence of the p.Ile61Asn variant, the extracellular loops of FSHR tend to adopt a nonparallel conformation, and their degree of twist increases, which could lead to misfolding (Figure 3a). As a rigid amino acid in terms of secondary structure, P688 contributes to maintaining the stability of the intracellular domain. However, the p.Pro688Thr variant becomes flexible and loose intracellularly, resulting in difficulty activating the downstream G-protein signaling pathway (Figure 3b). In short, both variants decrease FSHR activity in silico.

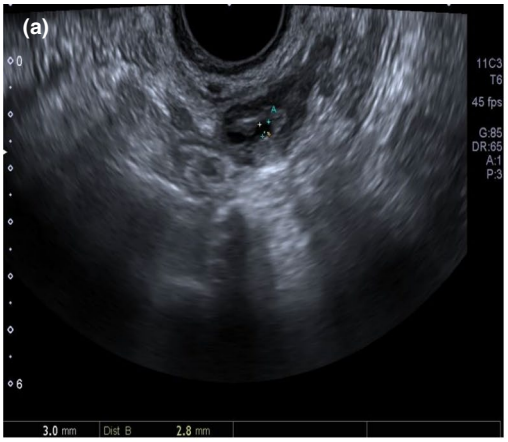

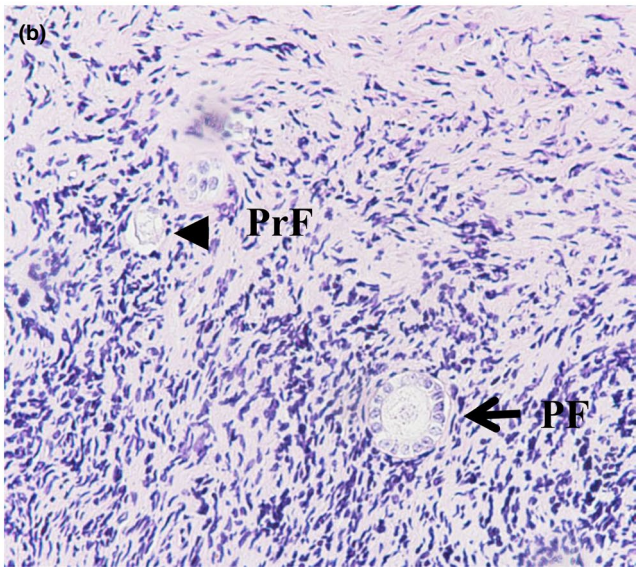

FIGURE 2 Ovarian structure of the proband. (a) Ultrasound scan of the ovary showing five early antral follicles (2–5 mm in diameter). Hematoxylin and eosin staining of the ovaries. (b) Section of the ovarian cortex containing three primordial follicles (PrFs) and one primary follicle (PF), indicated by arrowhead and arrow respectively (×200)

3.4 | Expression of FSHR and its variants in vitro

To demonstrate the functional changes in the p.Ile61Asn and p.Pro688Thr variants, the expression of wild-type FSHR and the p.Ile61Asn and p.Pro688Thr variants in HEK293T cells was determined by Western blotting. Cells transiently transfected with empty vector or vectors expressing wild-type, p.Ile61Asn, and p.Pro688Thr were harvested. The mature form of FSHR, approximately 87 kDa, was observed in cells expressing wild-type FSHR. Total FSHR protein expression was very similar in cells expressing wild-type FSHR or the p.Pro688Thr variant but was lower in those expressing the p.Ile61Asn variant (Figure 4a).

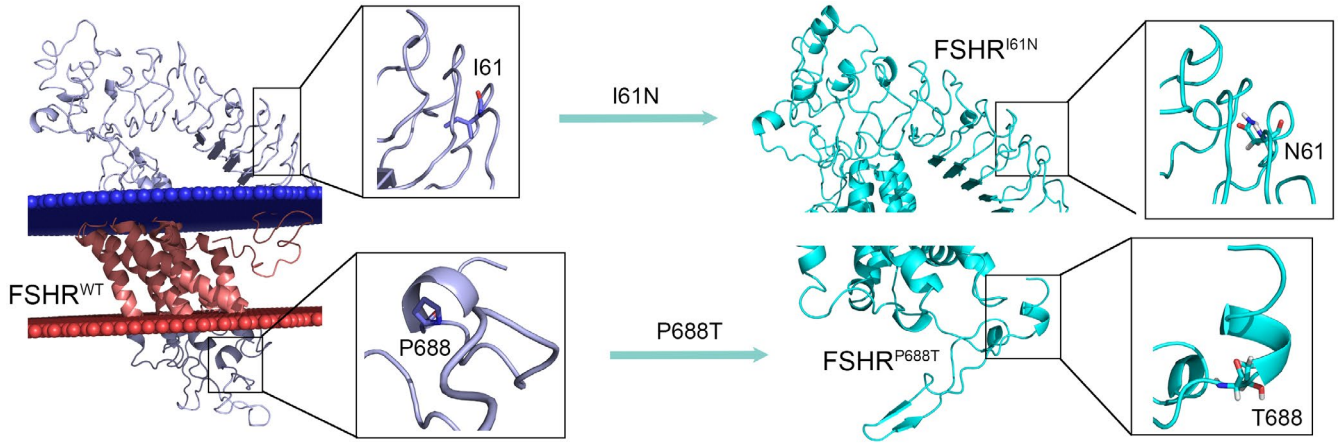

FIGURE 3 Cartoon representations of FSHR variant regions following 3-ns MD simulations. Left, wild-type FSHR embedded in the lipid bilayer. The membrane-binding region is shown in deep salmon, while the other regions are shown in light blue. The blue and red spheres represent the outer and inner sides of the membrane, respectively. Right, the extracellular domain of p.Ile61Asn (top) and the intracellular domain of p.Pro688Thr (bottom) are presented as cyan cartoons. In the magnified views, mutated residues are shown as sticks. The lipid membrane and water are omitted for clarity

3.5 | Functional analysis of the variants of FSHR

The surface localization of wild-type FSHR, p.Ile61Asn and p.Pro688Thr variants in HEK293T cells was detected by immunofluorescence. Confocal microscopy analyses demonstrated that the Flag tag was detectable in the cells transfected with wild-type FSHR, p.Ile61Asn, and p.Pro688Thr variants. As shown in Figure 4b, the p.Pro688Thr variant and wild-type FSHR displayed similar cell surface localization after 48 hr of transfection, but the p.Ile61Asn variant lost its membrane localization and was retained intracellularly.

FSH-induced signaling was measured based on FSH-induced cAMP production in HEK293T cells transfected with empty vector or vectors expressing wild-type FSHR, p.Ile61Asn or p.Pro688Thr variants and then stimulated with 0 (MOCK) or 500 IU/L FSH for 1 hr. The results showed an increase in cAMP production in cells harboring wild-type FSHR or p.Pro688Thr variant in response to FSH stimulation, but the cAMP increase was significantly lower in HEK293T cells expressing the p.Pro688Thr variant than in those expressing wild-type FSHR, indicating partial functional impairment of FSHR. In contrast, cAMP accumulation was not observed in cells expressing the p.Ile61Asn variant. These results showed that the p.Pro688Thr variant had partial functional impairment, while the p.Ile61Asn variant showed complete loss of FSHR activity (Figure 5).

4 | DISCUSSION

In this study, both the proband and her elder sister met the diagnostic criteria of ROS, having experienced hypergonadotropic hypoestrogenic amenorrhea before the age of 40 with high AMH values and small antral follicles (2–3 mm at ultrasonography). Whole-exome sequencing revealed compound heterozygous pathogenic *FSHR* variants (c.182T>A[p.Ile61Asn] and c.2062C>A[p.Pro688Thr]) in these patients. Thus, we identified two novel, pathogenic *FSHR* variants and performed complete clinical, endocrine, histological, and molecular analyses of the patients with these pathogenic *FSHR* variants.

FSHR is first expressed in granulosa cells as follicles progress from the primary to the secondary (preantral) stage. Histological analysis of Fshr−/− mouse ovaries shows follicular arrest before antral follicle formation. Consistent with this finding, the proband exhibited primordial follicles and primary follicles with granulosa cells but an absence of secondary follicles, corpora lutea, and mature Graafian follicles in ovarian biopsies. Both the proband and her elder sister presented a normal AFC by ultrasound scan, but the administration of exogenous human Gn failed to induce follicle development and ovulation. AMH is mainly produced by granulosa cells of growing ovarian follicles from the primary to the small antral stage. In this study, both the proband and her elder sister showed high AMH levels (7.07 and 13.84 ng/ml, respectively). These high AMH levels in patients with numerous primordial follicles and few primary follicles with granulosa cells indicate that FSHR is not necessary for AMH production or preantral follicle development. These results support the notion that AMH is secreted by small growing follicles.

FSHR is located on chromosome 2p21 and consists of 10 exons, which are transcribed into a protein of 695 amino acids that constitute all functional domains of FSHR. The two variants identified in this study are located in exon 2

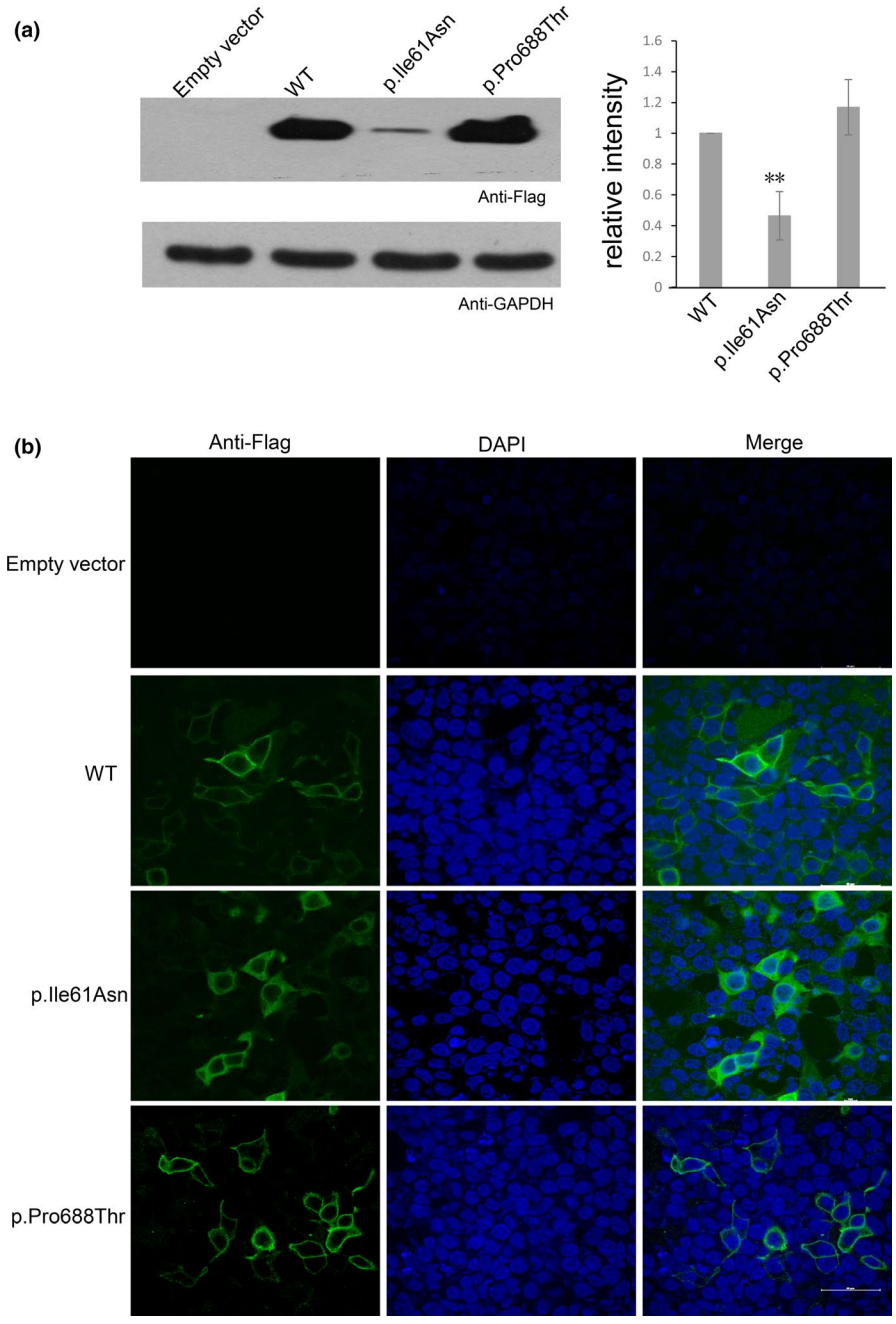

FIGURE 4 Expression of wild-type FSHR, p.Ile61Asn and p.Pro688Thr in HEK293T cells. (a) Western blot analysis determined the expression of wild-type (WT), p.Ile61Asn and p.Pro688Thr FSHR. GAPDH served as a loading control. Three experiments were performed with similar results, and statistical analysis of the relative intensity is shown on the right. $^{**}p < .01$. (b). The expression of WT, p.Ile61Asn and p.Pro688Thr FSHR in HEK293T cells was detected by immunofluorescence. Flag (green) was detected at the cell membrane in cells transfected with wild-type FSHR or the p.Pro688Thr variant but intracellularly in cells transfected with the p.Ile61Asn variant. Cell nuclei were counterstained with DAPI (blue)

(isoleucine to asparagine at position 61, p.Ile61Asn) and exon 10 (proline to threonine at position 688, p.Pro688Thr) of the FSHR, which encode the ECD and C-tail, respectively. The p.Ile61Asn variant is located in the ECD but alters the cell surface targeting of the receptor in vitro, leading to intracellular localization of the receptor. It is becoming well recognized that mutations of receptors, enzymes, and ion channels frequently result in protein misfolding and subsequent retention by chaperones of the cellular quality control system (Conn, Ulloa-Aguirre, Ito, & Janovick, 2007). Consistent with these results, two variants in the ECD of FSHR (p.Ile160Thr and p.Asp224Val) cause a defect in targeting to the cell surface (Beau et al., 1998; Touraine et al., 1999). According to the structures employed for MD simulations, the strongly polar N61 residue widens the distance between extracellular loops; thus, the p.Ile61Asn variant tends to result in a nonparallel conformation with an increased degree of twist, which could influence the folding of FSHR and impact its targeting to the cell surface.

The p.Pro688Thr variant is located in the intracellular tail of FSHR, where no variant had previously been reported in POI/ROS patients. These variants affect a rigid amino acid, causing the secondary structure of the intracellular domain to become flexible and loose intracellularly and disrupting its stability, resulting in impaired activation of the downstream G-protein signaling pathway. Confocal microscopy of p.Pro688Thr variant and wild-type FSHR

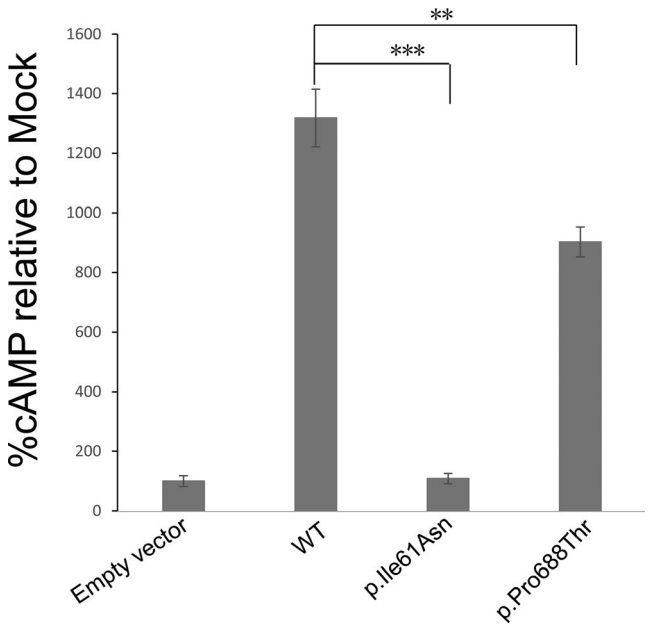

FIGURE 5 Cyclic adenosine monophosphate (cAMP) production stimulated by FSH in HEK293T cells. Cells transfected with the empty vector, wild-type FSHR or the p.Ile61Asn and p.Pro688Thr variants were stimulated with 0 (MOCK) or 500 IU/L FSH for 1 hr. Three experiments were performed with similar results. $^{**}p < .01$, $^{***}p < .001$

revealed similar cell surface localization. However, FSH-stimulated cAMP production by the p.Pro688Thr variant was significantly lower than that by wild-type FSHR. Although the p.Pro688Thr variant only disrupts some FSHR function, it is critical for the arrest of follicle development before the preantral follicle stage, as the proband's mother (I-2) was a heterozygous p.Ile61Asn variant carrier but had regular menses before 46 years of age and produced three offspring. Partial functional impairment of FSHR (p.Arg573Cys) was found in woman who had secondary amenorrhea and normal-sized ovaries with antral follicles up to 5 mm at ultrasonography (Beau et al., 1998). Recently, Matthew et al. also showed that a missense mutation (p.Asp408Tyr) in FSHR causes a decrease in cAMP production and leads to a POI phenotype with detectable AMH levels and primary follicles in both ovaries (Bramble et al., 2016). These studies suggest that limited FSH activity is sufficient to promote follicular growth up to the small antral stage but that further development requires strong FSH stimulation. The observed antral follicles and high AMH levels in the described patients might be due to partial functional impairment of FSHR (compound heterozygous variants: p.Ile61Asn and p.Pro688Thr).

To our knowledge, most pathogenic *FSHR* variants reported to date are located in the ECD and transmembrane domain, whereas no variants in the C-terminal domain have been reported in POI/ROS patients. The p.Pro688Thr variant is the first variant in the C-terminal domain of FSHR to be identified in POI/ROS patients, which indicates that the C-terminus of FSHR is also important for functional regulation. This result might improve the understanding of FSHR signal transduction.

In conclusion, we identified novel, inactivating compound heterozygous FSHR variants (p.Ile61Asn and p.Pro688Thr) in a pair of siblings affected by ROS. The p.Pro688Thr variant is the first identified in the C-terminus of FSHR. This observation suggests that follicular growth up to the small antral stage, as represented by AMH levels, can occur in the presence of impaired FSHR but that further development requires adequate FSH stimulation. We propose that patients diagnosed with ROS should be tested for FSHR variants.

ACKNOWLEDGMENTS

This study was supported by the National Natural Science Foundation of China (Nos. 81873856 and 81771533) and the Clinical Research Program of the 9th People's Hospital, Shanghai Jiao Tong University School of Medicine (JYLJ035).

CONFLICT OF INTEREST

The authors have declared no conflict of interest.

AUTHORS CONTRIBUTION

Dr. Lu and Dr. Kuang designed the study and contributed drafting the article. Dr. Khor contributed the functional analysis and data analysis. Dr. Lyu was responsible for the collection of data. All authors interpreted the findings and made critical revisions for important intellectual content.

ORCID

Xuefeng Lu https://orcid.org/0000-0002-8058-9630

REFERENCES

Aittomäki, K., Dieguez Lucena, J. L., Pakarinen, P., Sistonen, P., Tapanainen, J., Gromoll, J., … de la Chapelle, A. (1995). Mutation in the follicle-stimulating hormone receptor gene causes hereditary hypergonadotropic ovarian failure. *Cell*, *82*(6), 959–968. https://doi.org/10.1016/0092-8674(95)90275-9

Aittomaki, K., Herva, R., Stenman, U. H., Juntunen, K., Ylostalo, P., Hovatta, O., & de la Chapelle, A. (1996). Clinical features of primary ovarian failure caused by a point mutation in the follicle-stimulating hormone receptor gene. *Journal of Clinical Endocrinology and Metabolism*, *81*(10), 3722–3726. https://doi.org/10.1210/jcem.81.10.8855829

Allen, L. A., Achermann, J. C., Pakarinen, P., Kotlar, T. J., Huhtaniemi, I. T., Jameson, J. L., … Ball, S. G. (2003). A novel loss of function mutation in exon 10 of the FSH receptor gene causing hypergonadotrophic hypogonadism: Clinical and molecular characteristics. *Human Reproduction*, *18*(2), 251–256. https://doi.org/10.1093/humrep/deg046

Beau, I., Touraine, P., Meduri, G., Gougeon, A., Desroches, A., Matuchansky, C., … Misrahi, M. (1998). A novel phenotype related to partial loss of function mutations of the follicle stimulating

hormone receptor. *Journal of Clinical Investigation*, *102*(7), 1352–1359. https://doi.org/10.1172/JCI3795

Bramble, M. S., Goldstein, E. H., Lipson, A., Ngun, T., Eskin, A., Gosschalk, J. E., … Vilain, E. (2016). A novel follicle-stimulating hormone receptor mutation causing primary ovarian failure: A fertility application of whole exome sequencing. *Human Reproduction*, *31*(4), 905–914. https://doi.org/10.1093/humrep/dew025

Conn, P. M., Ulloa-Aguirre, A., Ito, J., & Janovick, J. A. (2007). G protein-coupled receptor trafficking in health and disease: Lessons learned to prepare for therapeutic mutant rescue in vivo. *Pharmacological Reviews*, *59*(3), 225–250. https://doi.org/10.1124/pr.59.3.2

Dickson, C. J., Madej, B. D., Skjevik, A. A., Betz, R. M., Teigen, K., Gould, I. R., & Walker, R. C. (2014). Lipid14: The amber lipid force field. *Journal of Chemical Theory and Computation*, *10*(2), 865–879. https://doi.org/10.1021/ct4010307

Dierich, A., Sairam, M. R., Monaco, L., Fimia, G. M., Gansmuller, A., LeMeur, M., & Sassone-Corsi, P. (1998). Impairing follicle-stimulating hormone (FSH) signaling in vivo: Targeted disruption of the FSH receptor leads to aberrant gametogenesis and hormonal imbalance. *Proceedings of the National Academy of Sciences of the United States of America*, *95*(23), 13612–13617. https://doi.org/10.1073/pnas.95.23.13612

Doherty, E., Pakarinen, P., Tiitinen, A., Kiilavuori, A., Huhtaniemi, I., Forrest, S., & Aittomaki, K. (2002). A Novel mutation in the FSH receptor inhibiting signal transduction and causing primary ovarian failure. *Journal of Clinical Endocrinology and Metabolism*, *87*(3), 1151–1155. https://doi.org/10.1210/jcem.87.3.8319

Feng, R., Sang, Q., Kuang, Y., Sun, X., Yan, Z., Zhang, S., … Wang, L. (2016). Mutations in TUBB8 and human oocyte meiotic arrest. *New England Journal of Medicine*, *374*(3), 223–232. https://doi.org/10.1056/NEJMoa1510791

Jiang, X., Liu, H., Chen, X., Chen, P.-H., Fischer, D., Sriraman, V., … He, X. (2012). Structure of follicle-stimulating hormone in complex with the entire ectodomain of its receptor. *Proceedings of the National Academy of Sciences of the United States of America*, *109*(31), 12491–12496. https://doi.org/10.1073/pnas.1206643109

Jo, S., Kim, T., Iyer, V. G., & Im, W. (2008). CHARMM-GUI: A web-based graphical user interface for CHARMM. *Journal of Computational Chemistry*, *29*(11), 1859–1865. https://doi.org/10.1002/jcc.20945

Jones, G. S., & De Moraes-Ruehsen, M. (1969). A new syndrome of amenorrhae in association with hypergonadotropism and apparently normal ovarian follicular apparatus. *American Journal of Obstetrics and Gynecology*, *104*(4), 597–600.

Kallio, S., Aittomaki, K., Piltonen, T., Veijola, R., Liakka, A., Vaskivuo, T. E., … Tapanainen, J. S. (2012). Anti-Mullerian hormone as a predictor of follicular reserve in ovarian insufficiency: Special emphasis on FSH-resistant ovaries. *Human Reproduction*, *27*(3), 854–860. https://doi.org/10.1093/humrep/der473

Katari, S., Wood-Trageser, M. A., Jiang, H., Kalynchuk, E., Muzumdar, R., Yatsenko, S. A., & Rajkovic, A. (2015). Novel inactivating mutation of the FSH receptor in two siblings of Indian origin with premature ovarian failure. *Journal of Clinical Endocrinology and Metabolism*, *100*(6), 2154–2157. https://doi.org/10.1210/jc.2015-1401

Kuechler, A., Hauffa, B. P., Koninger, A., Kleinau, G., Albrecht, B., Horsthemke, B., & Gromoll, J. (2010). An unbalanced translocation unmasks a recessive mutation in the follicle-stimulating hormone receptor (FSHR) gene and causes FSH resistance. *European Journal of Human Genetics*, *18*(6), 656–661. https://doi.org/10.1038/ejhg.2009.244

Lee, J., Cheng, X. I., Swails, J. M., Yeom, M. S., Eastman, P. K., Lemkul, J. A., … Im, W. (2016). CHARMM-GUI Input Generator for NAMD, GROMACS, AMBER, OpenMM, and CHARMM/OpenMM simulations using the CHARMM36 additive force field. *Journal of Chemical Theory and Computation*, *12*(1), 405–413. https://doi.org/10.1021/acs.jctc.5b00935

Liu, H., Xu, X., Han, T., Yan, L., Cheng, L., Qin, Y., … Chen, Z.-J. (2017). A novel homozygous mutation in the FSHR gene is causative for primary ovarian insufficiency. *Fertility and Sterility*, *108*(6), 1050–1055.e2. https://doi.org/10.1016/j.fertnstert.2017.09.010

Lomize, M. A., Pogozheva, I. D., Joo, H., Mosberg, H. I., & Lomize, A. L. (2012). OPM database and PPM web server: resources for positioning of proteins in membranes. *Nucleic Acids Research*, *40*(D1), D370–D376. https://doi.org/10.1093/nar/gkr703

Maier, J. A., Martinez, C., Kasavajhala, K., Wickstrom, L., Hauser, K. E., & Simmerling, C. (2015). ff14SB: Improving the accuracy of protein side chain and backbone parameters from ff99SB. *Journal of Chemical Theory and Computation*, *11*(8), 3696–3713. https://doi.org/10.1021/acs.jctc.5b00255

Nakamura, Y., Maekawa, R., Yamagata, Y., Tamura, I., & Sugino, N. (2008). A novel mutation in exon8 of the follicle-stimulating hormone receptor in a woman with primary amenorrhea. *Gynecological Endocrinology*, *24*(12), 708–712. https://doi.org/10.1080/09513590802454927

Touraine, P., Beau, I., Gougeon, A., Meduri, G., Desroches, A., Pichard, C., … Misrahi, M. (1999). New natural inactivating mutations of the follicle-stimulating hormone receptor: Correlations between receptor function and phenotype. *Molecular Endocrinology*, *13*(11), 1844–1854. https://doi.org/10.1210/mend.13.11.0370

Wang, J., Wolf, R. M., Caldwell, J. W., Kollman, P. A., & Case, D. A. (2004). Development and testing of a general amber force field. *Journal of Computational Chemistry*, *25*(9), 1157–1174. https://doi.org/10.1002/jcc.20035

Wu, E. L., Cheng, X., Jo, S., Rui, H., Song, K. C., Davila-Contreras, E. M., … Im, W. (2014). CHARMM-GUI membrane builder toward realistic biological membrane simulations. *Journal of Computational Chemistry*, *35*(27), 1997–2004. https://doi.org/10.1002/jcc.23702

Yang, J., Yan, R., Roy, A., Xu, D., Poisson, J., & Zhang, Y. (2015). The I-TASSER suite: Protein structure and function prediction. *Nature Methods*, *12*(1), 7–8. https://doi.org/10.1038/nmeth.3213

How to cite this article: Khor S, Lyu Q, Kuang Y, Lu X. Novel *FSHR* variants causing female resistant ovary syndrome. *Mol Genet Genomic Med*. 2020;8:e1082. https://doi.org/10.1002/mgg3.1082